Available online at www.sciencedirect.com

SciVerse ScienceDirect

Ceramics International 38 (2012) 4929–4933

CERAMICS INTERNATIONAL

www.elsevier.com/locate/ceramint

Fabrication, microstructure and mechanical properties of novel bulk binderless $(Ti_{0.8}Zr_{0.2})C$ carbides prepared by mechanical alloying and spark plasma sintering

A. Teber [a,b,*], F. Schoenstein [b], M. Abdellaoui [a], N. Jouini [b]

[a] *Laboratoire des matériaux utiles, Institut National de Recherche et d'Analyse Physico-chimique, Pôle technologique de Sidi Thabet, 2020 Sidi Thabet, Tunisia*

[b] *Laboratoire des Sciences des Procédés et des Matériaux, CNRS-UPR 9001, Université Paris 13, PRES Sorbonne Paris Cité, 93430 Villetaneuse, France*

Received 26 June 2011; received in revised form 20 February 2012; accepted 27 February 2012
Available online 23 March 2012

Abstract

Nanocrystalline $(Ti_{0.8}Zr_{0.2})C$ powder consisting in grains of about 200 nm in diameter obtained by mechanical alloying was sintered by a spark plasma sintering (SPS) process without the addition of any binder phase. The microstructure, Vickers micro hardness and density in relation to the sintering time and temperature are carefully described. The most suitable sintering condition under pressure of 50 MPa is 1650 °C for 5 min. In this sintering condition, the hardness can reach 2760 Hv and the relative density can reach 98%.

Keywords: B. Microstructure; C. Mechanical properties; C. Hardness; Binderless $(Ti_{0.8}Zr_{0.2})C$; Spark plasma sintering; Density

1. Introduction

Hard materials, such as TiC–Ni cermet, where Ni is a binder phase, have long been used as cutting tools, dies and wear resistant parts, owing to their high level of hardness and excellent wear resistance as well as their retention of room temperature hardness at elevated temperatures [1].

In our previous work [2], we synthesized a new compound $(Ti_{0.8}Zr_{0.2})C$ which is a new hard material as we expected. Practically, $(Ti_{0.8}Zr_{0.2})C$ consists in replacing Ti by Zr in TiC. The as-obtained solid solution crystallizes in the fcc space group Fm-3m, and has the TiC type structure. The cell parameter of $(Ti_{0.8}Zr_{0.2})C$ is $a = 0.4332$ nm. Considering that $(Ti_{0.8}Zr_{0.2})C$ is isostructural with TiC, we assume that the sinterability of $(Ti_{0.8}Zr_{0.2})C$ may be similar to that of TiC.

The densification of conventional TiC powder usually occurs in the liquid phase sintering through the addition of 20–60 wt.% of metallic binder usually from Ni or Mo [1,3].

The binder phase facilitates the sintering to a full-density bulk, and controls the bonding between TiC particles and increases the toughness of the sintered bulk [4]. However, addition of the binder phase not only decreases hardness and corrosion/oxidation resistance of the materials but also causes heat stress due to the difference between the thermal expansions of TiC compared to that of the binder phase. Because of the high-melting point of TiC, however, it is relatively difficult to sinter pure TiC without any binder phase using a conventional process in which the liquid phase is partly necessary during the sintering process.

The spark plasma sintering (SPS) process has attracted considerable attention because of its high pressure and rapid sintering at a relatively low temperature in comparison with the conventional sintering process. The use of the (SPS) process to successfully consolidate carbide powders without a binder has been demonstrated in several investigations [5]. Therefore, in order to obtain the well sintered specimen with a high level of hardness, we aimed to sinter ultrafine pure $(Ti_{0.8}Zr_{0.2})C$ with

* Corresponding author at: Laboratoire des Sciences des Procédés et des Matériaux, CNRS-UPR 9001, Université Paris 13, PRES Sorbonne Paris Cité, 93430 Villetaneuse, France. Tel.: +33 149 40 34 95; fax: +33 14 94 03 938.
E-mail address: teber.esstt@gmail.com (A. Teber).

0272-8842/$36.00
doi:10.1016/j.ceramint.2012.02.085

almost full densification using the SPS process without any binder metal, which is expected to have excellent properties. The microstructure, Vickers micro hardness and density are carefully described.

2. Experimental

2.1. Synthesis of the powder

The mixture of elemental Ti (<40 μm, 99.9%, Prolabo), carbon (99.9%, Fischer scientific) and zirconium (99.9%, ACROS) is sealed into a stainless steel vial (45 ml in volume) with 5 stainless steel balls (15 mm in diameter and 14 g in mass) in a glove box filled with argon gas. The ball-to-powder weight ratio was about 70 to 1. The mechanical alloying procedure was performed at room temperature using a planetary ball mill (Fritsch pulverisette 7) with milling conditions corresponding to 7.41×10^{-2} J/hit kinetic shock energy, 70.1 Hz shock frequency and 5.19 W/g injected shock power [6,7].

2.2. Consolidation of the powder

The consolidation process of nanometric $(Ti_{0.8}Zr_{0.2})C$ carbide was realized by a spark plasma sintering (SPS)-515S SYNTEX apparatus. The power supply produces a pulsed DC current, reaching 720 A at 3 V. The pulse pattern used in this work was 12:2, i.e., 12 pulses on and 2 pulses off. Each pulse has a duration of about 3.3 ms. Temperatures were measured by a pyrometer focused on the surface of the graphite die. Sintering was done in a vacuum of 19 Pa in a graphite die with an inside diameter of 8 mm, an outside diameter of 45 mm and a height of 36 mm. The densities of the consolidated samples were measured by the Archimedes method using O-xylene as measuring liquid (0.88 density at 25 °C).

2.3. Characterization techniques

XRD patterns of the synthesized powders were obtained using a (θ–2θ) Panalytical XPERT PRO MPD diffractometer operating with CoKα radiation (λ = 0.17890 nm). The existing phases were determined using the ICDD PDF2 database. The same XRD patterns were analyzed by the Fullprof program [8] based on the Rietveld method [9] in order to determine the cell parameters, the mean diffraction crystallite size (DCS) and the weight content of each existing phase in the synthesized alloy.

Sintered samples were ground with a diamond wheel and then carefully ground and polished. The morphology and the average diameter of the initial $(Ti_{0.8}Zr_{0.2})C$ particles were observed by using a JEOL-2011 transmission electron microscope (TEM) operating at 200 kV. The microstructures of fractured samples were observed by scanning electron microscopy (SEM). Micro-hardness measurements were conducted on the perpendicular plane to the pressing direction using a Duramin 20 Vickers device with a test force of 1.916 N during 10 s.

3. Result and discussion

3.1. X-ray diffraction characterization

Fig. 1 shows the XRD pattern of the $(Ti_{0.8}Zr_{0.2})C$ bulk alloy obtained at 1650 °C and 50 MPa for 5 min. The peaks of the $(Ti_{0.8}Zr_{0.2})C$ phase still occur, confirming that the pure phase does not undergo a decomposition process in this condition. Zr is still dissolved in a Ti lattice after being sintered, since no peaks of Zr and/or zirconium compounds are observed in the XRD pattern. This suggested that the new solid solution $(Ti_{0.8}Zr_{0.2})C$ has excellent thermal stability even up to 1650 °C during spark plasma sintering. The broadening of the diffraction lines of the consolidated samples decrease in $(Ti_{0.8}Zr_{0.2})C$ in comparison with those of the previous powder, which indicates an increase in the crystallite size. Calculating the average crystallite size based on the width of the $2\theta = 36.32^\circ$ diffraction peak by Scherrer's formula results in values of 73 nm. Starting from a peak intensity analysis, using the Match program [10], the as-obtained material is practically constituted of a pure phase $(Ti_{0.8}Zr_{0.2})C$. The calculated lattice parameter based on the X-ray data in Fig. 1 is $a = 0.4335$ nm which is slightly larger than that of TiC (0.4327 nm) [11].

3.2. Densification behavior and microstructure

The sintering behavior of the $(Ti_{0.8}Zr_{0.2})C$ sample is presented in Fig. 2(a) and (b). The theoretical density of $(Ti_{0.8}Zr_{0.2})C$ is 5.13 g cm^{-3}. The variation of the density of the samples sintered at different temperatures for 5 min and 50 MPa is shown in Fig. 2(a). The density of $(Ti_{0.8}Zr_{0.2})C$ increased along with the increase in sintering temperature and reached maximum value (98% of theoretical density) at 1650 °C. At higher temperatures, a diminution in density was

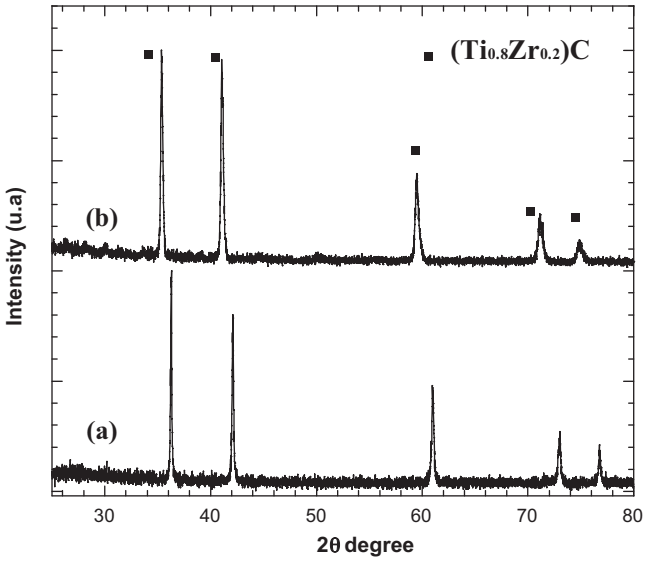

Fig. 1. XRD patterns of as-elaborated $(Ti_{0.8}Zr_{0.2})C$ powder (a) and dense samples (b).

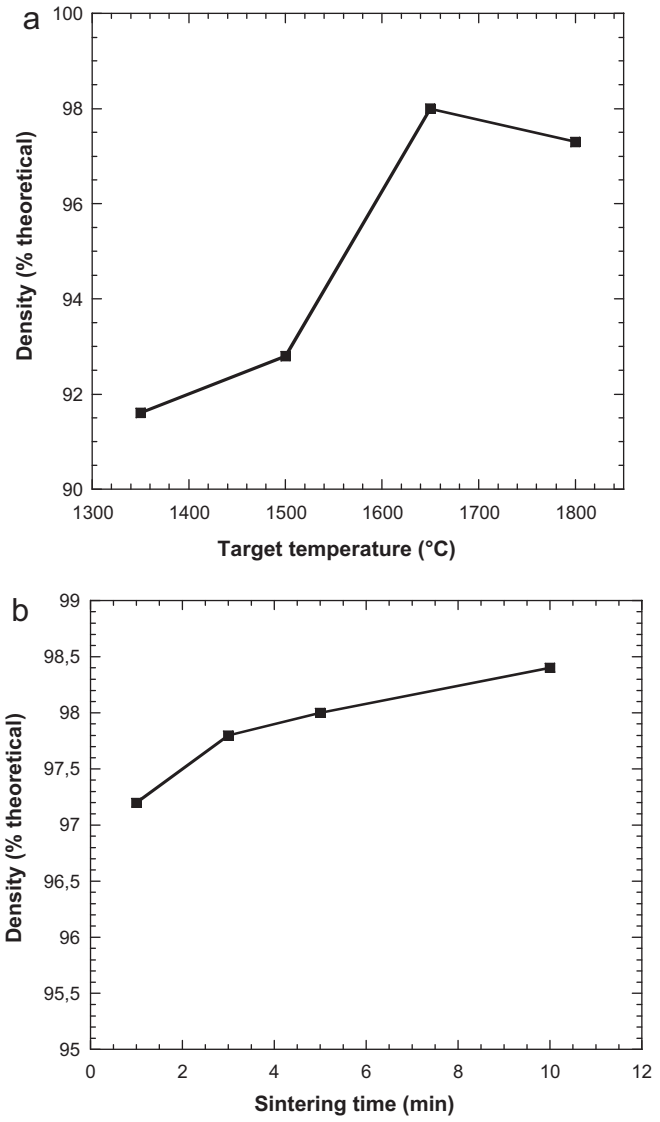

Fig. 2. (a) The relative density of various sintered samples vs. sintering temperature for 5 min and (b) the relative density of various sintering time at 1650 °C.

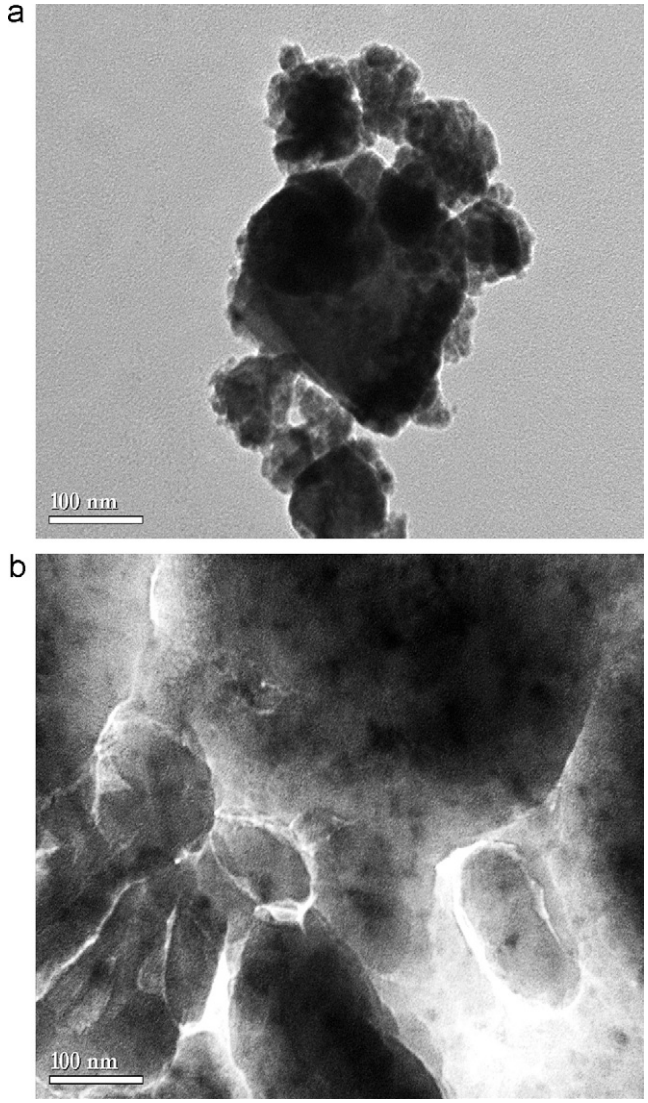

Fig. 3. TEM images from: (a) the initial $(Ti_{0.8}Zr_{0.2})C$ powder, (b) sintered sample at 1650 °C and 50 MPa for 5 min.

observed, which could be due to the inhomogeneous grain growth, inducing strain and cracks in the sample microstructures [12]. Thus, the optimum sintering temperature was estimated to be 1650 °C.

Fig. 2(b) shows the relative density of various samples sintered at 1650 °C vs. sintering time. The density increased with the increase in the holding time. As concerns the samples sintered for 5 min, the relative density was over 98%. The relative density of binderless $(Ti_{0.8}Zr_{0.2})C$ can reach 98.6% after sintering at 1650 °C for 8 min.

The microstructure of the sample was observed by the SEM and TEM. In fact, the TEM micrograph of the powder before sintering roughly shows particles of spherical morphology with a diameter ranging from 100 to 200 nm (Fig. 3a). The difference between the particles' diameter given by the TEM and the crystallites' size calculated from the X-ray pattern suggests that the $(Ti_{0.8}Zr_{0.2})C$ particles are formed through an aggregation growth process. As concerns the consolidated samples (Fig. 3b), it can be clearly observed that the SPS consolidation process induces no significant change in the particles' morphology, but an increase in the grains' size could be clearly noted. The grains' diameter increased to about 700 nm which clearly indicates that the SPS process limits the grain growth during sintering unlike the conventional sintering process.

Fig. 4 shows SEM images of polished and fracture samples consolidated at 1650 °C, 50 MPa and at different times. As shown in Fig. 4a, a group of small pores were observed in $(Ti_{0.8}Zr_{0.2})C$ carbide sintered at 1 min. When the sintering time was 5 min, small pores are observed. In fact, the intergranular pores coalesced to form closed pores. Particles of different sizes agglomerate to form coarse grains, while heterogeneous distribution of equiaxed grains still occurs. Fig. 4b and d shows that the fracture mode is mostly transgranular.

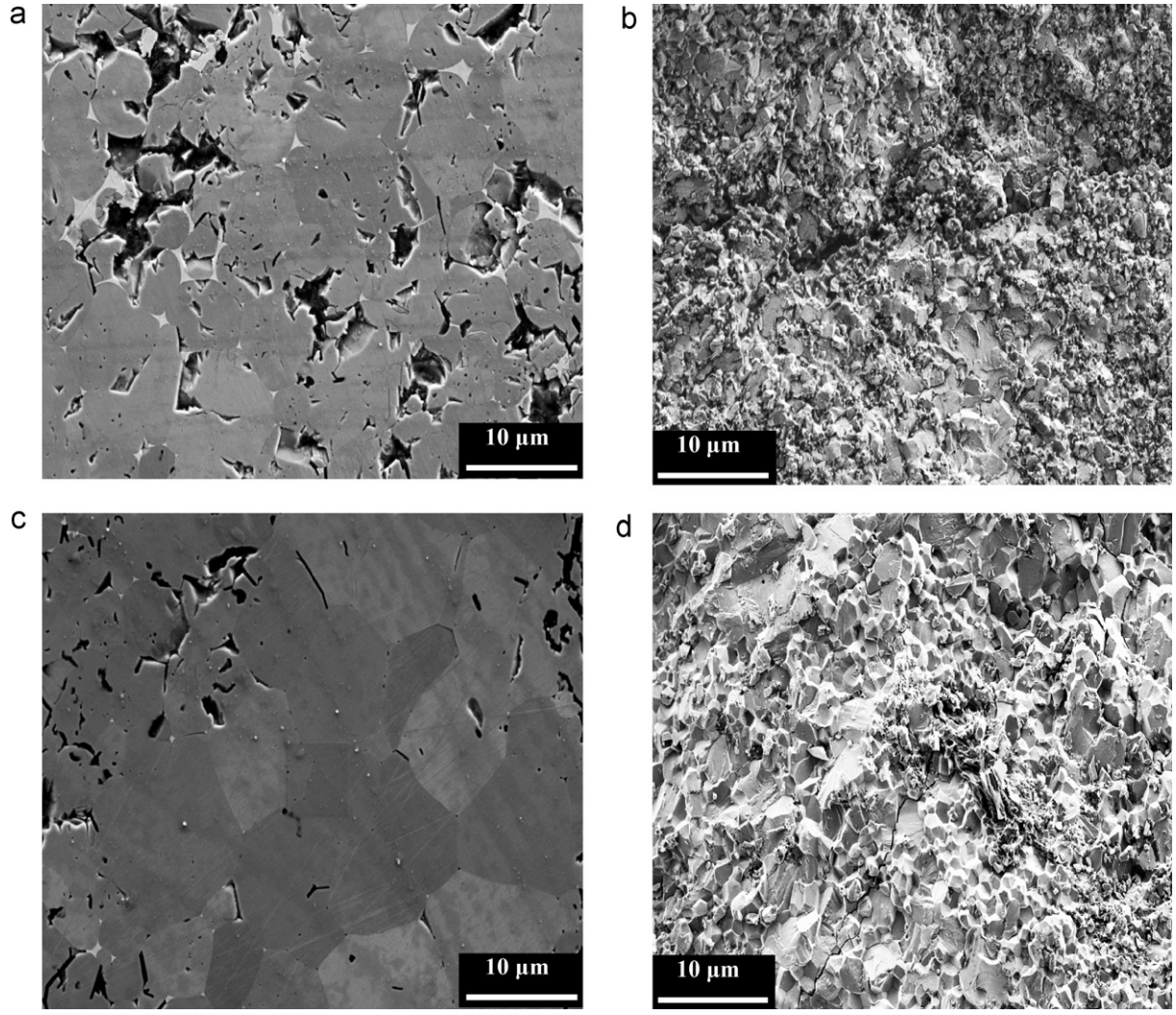

Fig. 4. SEM micrographs of $(Ti_{0.8}Zr_{0.2})C$ powder sintered at different holding times; (a) and (b) at 1 min; (c) and (d) at 5 min. (a and c: polished surfaces) and (b and d: fracture surfaces).

3.3. Mechanical properties

Fig. 5 shows the variation of hardness according to sintering temperature. The hardness could be affected by both relative density and grain size. Pores in ceramics have no resistance to applied stress, so materials of higher porosity have lower apparent hardness than dense materials. In addition to the effects of porosity, the grain size also influences hardness. Smaller grain size increases the frequency with which dislocations encounter grain boundaries, thus requiring larger stresses for deformation to occur [13]. In our study, part of the increase in hardness observed when there is an increasing relative density could be explained by the relative density effect. Increasing the temperature from 1650 °C to 1800 °C, the hardness decreased slightly from 2760 Hv to 2650 Hv caused by the grain growth of $(Ti_{0.8}Zr_{0.2})C$ and the formation of abnormally large grains, consistent with observations reported by others [13,14]. Le Flem et al. [15] reported a lower hardness value of 2200 Hv for TiC obtained by hot isostatic pressing. We assume that this difference is due to the high relative density of

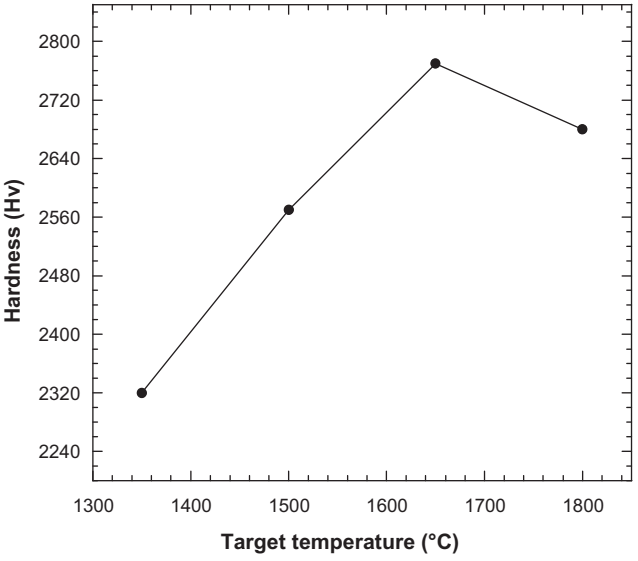

Fig. 5. The Vickers hardness of various sintered samples vs. sintering temperature.

the material obtained after being consolidated by SPS in optimum conditions in the cited work.

4. Conclusions

In this work, bulk binderless $(Ti_{0.8}Zr_{0.2})C$ carbides were prepared by mechanical alloying and spark plasma sintering. The sintered $(Ti_{0.8}Zr_{0.2})C$ carbides exhibit excellent physical and mechanical properties. The conclusions of this study are as follows:

- The sintering temperature rather than the sintering time, appears as the most important factor governing the hardness, density and microstructure of the sintered specimen.
- The optimized set of sintering parameters is a particle diameter of 0.7 μm, a sintering temperature of 1650 °C and a hold time of 5 min; the density of the product is 98% and the Vickers micro-hardness of the material reaches 2760 Hv.
- The new solid solution $(Ti_{0.8}Zr_{0.2})C$ has excellent mechanical properties, although when 20% zirconium is dissolved in the titane, the hardness of $(Ti_{0.8}Zr_{0.2})C$ (2760 Hv) is greater than that of normal hard alloying TiC (2200 Hv). Considering the high level of hardness, and the lower density, the as-obtained solid solution is expected to replace the standard materials for cutting tools, and wear-resistance parts and so on.

Based on these results, we conclude that the sintered $(Ti_{0.8}Zr_{0.2})C$ carbides described herein, and the above method of powder production have considerable potential for use in structural applications.

Acknowledgment

We would like to express our thanks to J. Morrice-Abrioux (IUT Saint-Denis, Université Paris 13) for careful reading of the manuscript.

References

[1] Y. Lia, P. Baia, Y. Wangb, J. Hub, Z. Guob, Effect of Ni contents on the microstructure and mechanical properties of TiC–Ni cermets obtained by direct laser fabrication, Int. J. Refract. Met. Hard Mater. 27 (2009) 552–555.
[2] C. Slama, A. Teber, M. Abdellaoui, Synthesis and characterization of $Ti_{1-x}Zr_xC$ rich nano-composite, Phys. Chem. News 54 (2010) 90–94.
[3] J. Pirso, M. Viljus, S. Letunovits, Sliding wear of TiC–NiMo cermets, Tribol. Int. 37 (2004) 817–824.
[4] H.E. Exner, Physical and chemical nature of cemented carbides, Int. Metals Rev. 4 (1979) 149–173.
[5] J. Zhao, T. Holland, C. Unuvar, Z.A. Munir, Sparking plasma sintering of nanometric tungsten carbide, Int. J. Refract. Met. Hard Mater. 27 (2009) 130–139.
[6] M. Abdellaoui, E. Gaffet, A mathematical and experimental dynamical phase diagram for ball-milled $Ni_{10}Zr_7$, J. Alloys Compd. 209 (1994) 351–361.
[7] M. Abdellaoui, E. Gaffet, The physics of mechanical alloying in a planetary ball mill: mathematical treatment, Acta Metall. Mater. 433 (1995) 1087–1098.
[8] Rodriguez-Carvajal, Recent advances in magnetic structure determination by neutron powder diffraction, J. Phys. B 192 (1993) 55–69.
[9] H.M. Rietveld, A profile refinement method for nuclear and magnetic structures, J. Appl. Crystallogr. 2 (1969) 65–71.
[10] K. Brandenburg, H. Putz, Match: phase identification from powder diffraction, (C) 2003–2009 Crystal IMPACT.
[11] M. Sherif El-Eskandarany, Structure and properties of nanocrystalline TiC full-density bulk alloy consolidated from mechanical reacted powders, J. Alloys Compd. 305 (2000) 225–238.
[12] M.C. Steil, J. Fouletiera, M. Kleitza, P. Labrune, BICOVOX: sintering and grain size dependence of the electrical grain size dependence of the electrical properties, J. Eur. Ceram. Soc. 19 (1999) 815–818.
[13] T. Li, Q. Li, J.Y.H. Fu, P.C. Yu, L. Lu, C.C. Wu, Effects of AGG on fracture toughness of tungsten carbide, Mater. Sci. Eng. A 445 (2007) 587–592.
[14] Y. Zhao, L.J. Wang, G.J. Zhang, W. Jian, Li D. Chen, Effect of holding time and pressure on properties of ZrB–SiC composite fabricated by the spark plasma sintering reactive synthesis method, Int. J. Refract. Met. Hard Mater. 27 (2009) 177–180.
[15] M. Le Flem, A. Allemand, S. Urvoy, D. Cédat, C. Rey, Microstructure and thermal conductivity of Mo–TiC cermets processed by hot isostatic pressing, J. Nucl. Mater. 380 (2008) 85–92.